King Fahd University of Petroleum and Minerals

Department of Physics

PHYS 503 - Graduate Laboratory Report

Term 152

Boron Concentration Measurement in Water Sample using $CeBr_3$ detector

Abul Lais (g201409280)

Course Instructor: Dr A. A. Naqvi

A Report submitted to the Department of Physics, King Fahd University of Petroleum and Minerals, in partial fulfillment of the requirements for the course of

Physics 503: Graduate Laboratory

27 February 2016

Keywords: Prompt Gamma Activation Analysis, Standard Boron solution, boron neutron capture theory, $CeBr_3$ scintillation detector, low-energy gamma applications

Abstract

A new $CeBr_3$ detector was tested for reliable performance using a portable neutron generator-based PGNAA (Prompt Gamma Neutron Activation Analysis) set-up on 6 boron-contaminated water samples containing boron concentrations of 0.03125 – 0.25 wt% conc. From the difference between the boron sample spectrum and the detector's background spectrum, the difference spectra were extracted. The integrated yield of boron peak in each sample difference spectrum was assumed to be proportional to the boron concentration in the corresponding water sample. A linear regression was fitted between net boron peak integrated yield and the corresponding boron concentration in water sample and a correlation coefficient of R = 0.98 was obtained. This verifies the excellent performance of the $CeBr_3$ detector, for detection of boron in water sample.

Table of Contents

1. Introduction

Prompt Gamma Neutron Activation Analysis (PGNAA) is a widely-applicable materials characterization technique for determining the elemental composition of a target sample, and is used for analysing samples of the order of micrograms to kilograms. The bulk of the applications of PGNAA is in nondestructive elemental analysis of matter. Very often, owing to a variety of causes, it is essential to know what the composition of a sample is i.e. what is the percentage of each element within a sample. Such situations often arise in testing samples for harmful radioactive or toxic contaminants in food, soil or even bricks. PGNAA is a swift and efficient technique in such situations.

Basic principles of PGNAA

The basic principles of PGNAA is illustrated in Figure 1. The sample is irradiated with an incident neutron beam. The elements within the sample absorb these neutrons, to form a short-lived excited metastable nuclide, which instantaneously decays to the ground state by the prompt emission of gamma rays. These are measured with a detector known as a gamma ray spectrometer, which gives a spectral graph output. At this point, what remains is a ground-state radioactive nucleus, which slowly decays over its characteristic half-live by beta- and delayed gamma-emission to form a stable daughter nucleus [1].

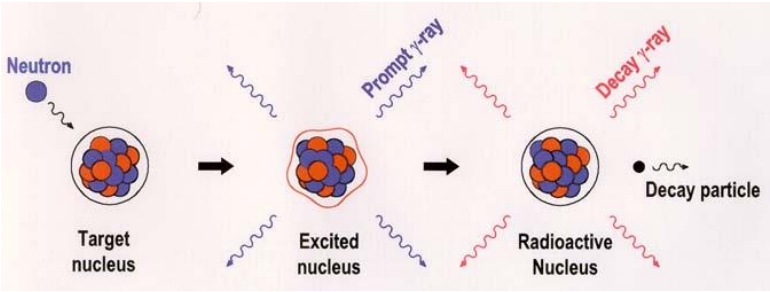

Figure 1: PGNAA and NAA decay scheme

It is crucial to understand the difference between prompt-gamma activation analysis (PGNAA) and its closely-related associate, neutron activation analysis (NAA). With reference to Figure 1, NAA would analyze the decay gamma ray [2] whilst PGNAA would study the prompt gamma ray. This also highlights three advantages of PGNAA over NAA; some elements do not form neutron capture products, rendering them unsuitable for NAA but PGNAA still works even if no new nuclides are formed, but simply excited versions of the original nuclide. Hence, nuclear transformation is always accompanied by (prompt) gamma radiation unless the nucleus is formed directly in the ground state, an unlikely event. In addition, PGNAA is a non-destructive technique

so it can be used for sensitive samples, such as biological ones, where maintaining sample integrity is important. Lastly, the recording time for PGNAA is much shorter than NAA, which saves time [3]. NAA occurs over the standard half-life of the nuclide, which may range from minutes to even days. In contrast PGNAA utilizes the prompt gamma rays emitted by the excited metastable product, well before it undergoes any radioactive decay. This is the way the final nucleus releases the excitation energy gained in the reaction, and the time scale is of order 10^{-15} s. Hence, in cases where getting results swiftly is a priority, PGNAA is clearly the advantageous method.

Within PGNAA set-up, the neutrons are produced by a neutron generator that uses nuclear fusion of 2 deuterium atoms as per:

$$D + D \rightarrow n + {}^{3}He \qquad E_n = 2.5 \text{ MeV}$$

where by accelerating a deuteron to a few hundred keV of energy and hitting onto a deuterium target, fusion of deuterium atoms (D + D) results in the above reaction with the production of a neutron with a kinetic energy of approximately 2.5 MeV.

However, these neutrons are fast neutrons with low capture cross-section so a polyethylene moderator (having high density of atomic hydrogen) slows them down until they become slow-moving thermal neutrons. Hydrogen has almost the same mass as neutrons so linear momentum conservation ensures maximum energy loss from and slowing down of the neutrons, and thus high thermal neutron generation rate. The basic collision theory states that if a moving mass collides into a stationary mass, energy loss from the first mass is maximized if the 2 masses are the same, based on the energy-loss equation given below [4]:

$$\frac{E_{R|max}}{E_n} = \frac{4A}{(1+A)^2}$$

where A is the mass of the moderator nucleus, E_n is the energy of the incident neutron and $E_{R|max}$ is the maximum possible energy loss from the recoiling moderator nucleus. We want to maximize the ratio $\frac{E_{R|max}}{E_n}$, under which circumstance the emergent neutron has the lowest energy (and speed), thus producing thermal neutrons, and calculus yields A = 1 as the condition for $\frac{d}{dA}\left(\frac{E_{R|max}}{E_n}\right) = 0$. So the condition A = 1 implies that the best moderator has mass number of 1, which explains why hydrogen is an ideal neutron moderator.

For this study, we used PGNAA technique to analyse boron-contaminated water samples since its use as a binary radiation therapy is well known for treating cancerous cells using Boron

Neutron Capture Theory (BNCT) [5]. Binary modality brings together two components that when kept separate have only minor effects on healthy cells. The two are boron-10 that can be concentrated in tumor cells by attaching it to tumor seeking compounds, and a beam of thermal neutrons. Boron-10 in or adjacent to the tumor cells disintegrates after capturing a neutron and the high energy heavy charged particles produced destroy only the cells in close proximity to it, primarily cancer cells, leaving adjacent normal cells largely unaffected. Hence, studying boron is not only an academic exercise but of tremendous practical benefits in the cancer treatment sector [5].

The boron samples were analysed using a $CeBr_3$ detector. In the field of gamma ray detection, the primary issue is the detection of low intensity gamma-ray emissions. For instance these may arise from planetary surface emissions, or from detection of trace amounts of illegal nuclear material. In such cases, amongst others, the count rate is often extremely low hence the detector should have high detection sensitivity. $LaBr_3$:Ce(5%Ce) offers some advantages in terms of ease-of-use and high-energy resolution over NaI(Tl) and HPGe detectors respectively. However, the intrinsic activity of ^{138}La partially spoil its detection performance, particularly for energies below 1.5MeV, because it is naturally radioactive. In other words, lanthanide detectors are not very suitable for detection in the low-energy window. As shown by Schotanus et al [6] "$CeBr_3$ is an optimum compromise between an ideal ^{138}La-free-$LaBr_3$:Ce(5%Ce) and $LaBr_3$:Ce(5%Ce) itself, offering concrete advantage over $LaBr_3$:Ce(5%Ce) for the detection of low intensity gamma rays." This advantage is due to both cerium and bromine not being naturally radioactive, which makes them suitable for low-energy applications. Hence, a $CeBr_3$ detector was chosen for this present study.

2. Objectives of the study

We have acquired a new $CeBr_3$ detector and would like to test its performance for detection of boron concentration in contaminated water samples. If the detector yields a linear relationship, it verifies the reliable performance of the $CeBr_3$ detector. For this purpose, we used a portable neutron generator-based PGNAA set-up [7] that is described in the following section.

3. Experimental setup

The geometry of the 2.5 MeV-based PGNAA set-up [7] is shown in Figure 2. The main components are: MP320 Thermoscientific portable neutron generator, cylindrical polyethylene moderator, 76 mm x 76 mm $CeBR_3$ scintillation detector for gamma-ray detection, together with lead and paraffin shielding.

The MP320 portable neutron generator radiates a stream of 2.5 MeV neutrons by the D + D fusion reaction. A (70keV, 70 μA) deuteron beam is irradiated against a stationary deuterium target to carry out the fusion. At 2.5 MeV, the neutrons are fast neutrons, with small neutron capture cross-section. These fast neutrons from the generator are slowed down by polyethylene (high atomic hydrogen density) moderator to yield thermal neutrons, which have large neutron capture cross-section. A cylindrical cavity of radius X mm has been drilled through the moderator so that a cylindrical sample can be tested by PGNAA. Unwanted neutrons and stray gamma-rays is obstructed from entering the detector using 3 mm thick lead shielding and 50 mm thick paraffin shielding. The detector is high-sensitivity $CeBr_3$ gamma-ray spectrometer supplied by Scionix Holland BV.

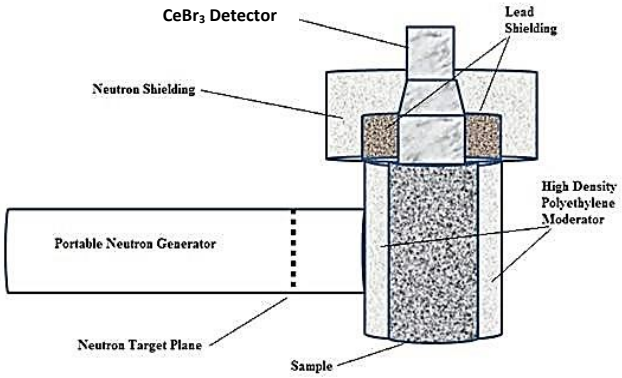

Figure 2: PGNAA experimental set-up

To prepare the boron-contaminated water samples, we used 3 bottles of standard boron solution rated at 0.03125, 0.125 and 0.25 wt% conc. that were present in our laboratory. In addition, a further 2 bottles rated at 0.0833 and wt% conc. were prepared by diluting 0.25 wt% conc. solution with distilled water in the correct stoichiometric proportion. The bottles were then dried with tissue paper to avoid contamination and weighed on a mass balance as follows:

Boron concentration (wt% conc.)	Mass (g)
0.03125	709
0.0833	671
0.125	705
0.167	676
0.25	699

Table 1: Total mass of boron-contaminated water samples (including bottle)

Boron was detected through the 478 keV gamma ray emitted when it was irradiated with thermal neutrons, leading to following reaction:

$$^{10}B + n \longrightarrow {}^{11}B^*$$

$$^{11}B^* \longrightarrow {}^{7}Li + {}^{4}He + \gamma(478\ keV)$$

In brief, the ^{10}B atoms within the sample undergoes thermal neutron capture that lead to the formation of a short-lived unstable ^{11}B isotope that decays spontaneously to form the stable $^{7}_{3}Li$ nuclide, simultaneously emitting a 478 keV gamma ray. The energy-level decay scheme that leads to the abovementioned emitted gamma ray is as follows:

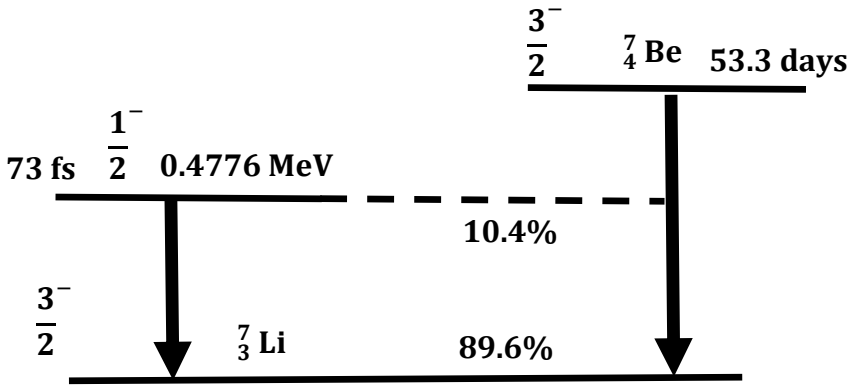

Figure 3: Nuclide decay scheme showing production of 478 keV gamma photon

After preparing the boron-contaminated water samples, all the bottles were shaken thoroughly to ensure a homogeneous mixture was formed. This shaking step was repeated before loading the samples into the detector cavity for testing. Prior to testing, to ensure safety to personnel, the main experimental room (where the neutron generator is) was securely locked before switching on the neutron beam. A +700V bias voltage was applied to the detector during the experimentation.

The $CeBr_3$ detector displays the output in the form of an intensity vs channel number plot that is displayed on a computer. These are the general steps in our experimental set-up. Next, there are

3 parts in the current study – measuring the detector intrinsic spectrum, the detector activation spectrum and the boron sample spectrum, which are detailed in the forthcoming sub-sections.

3.1 $CeBr_3$ Detector and its Activation Spectrum

3.1.1 Intrinsic spectrum

The naturally-radioactive isotopes present in the detector material emit gamma rays, which constitutes the intrinsic spectrum. To measure the intrinsic spectrum of the $CeBr_3$ detector, the neutron beam was switched off, and no sample was placed in the cavity. Hence, the detector only detected the presence of naturally-occurring radioisotopes present in the detector. The run time was approximately 1500s.

The intrinsic spectrum of our $CeBr_3$ detector is shown in Figure 3. In general, it shows an exponentially-decreasing intensity profile modulated with impurity radioisotope peaks, which is in agreement with theoretical predictions since there is generally less random background radiation at higher energies than lower energies. However, this smoothly-decaying profile is interrupted by prominent intrinsic peaks that correspond to the decay energies of various natural radioisotopes present in the detector. From Schotanus et al [6], we learn that Ce and Br elements do not present any naturally occurring radioisotopes, and the reason for intrinsic activity is the ^{227}Ac radioactive impurities present in the raw materials used for the detector. They attribute this contamination to the homologous nature of Ac and Ce, which makes it extremely difficult to separate them from one another, hence the cerium would be contaminated with trace amounts of actinium. This is indeed observed in Figure 3, which shows intrinsic gamma ray activity spectrum of the $CeBr_3$ detector over the 0 – 2500 keV energy range. This spectrum was taken with amplifier gain settings (coarse gain = 20, fine gain = 8.00) that allow the full spectrum to be recorded as the peaks of interest are in the high-energy region at 1510, 1750 and 1990 keV due to ^{227}Ac contamination in the $CeBr_3$ detector.

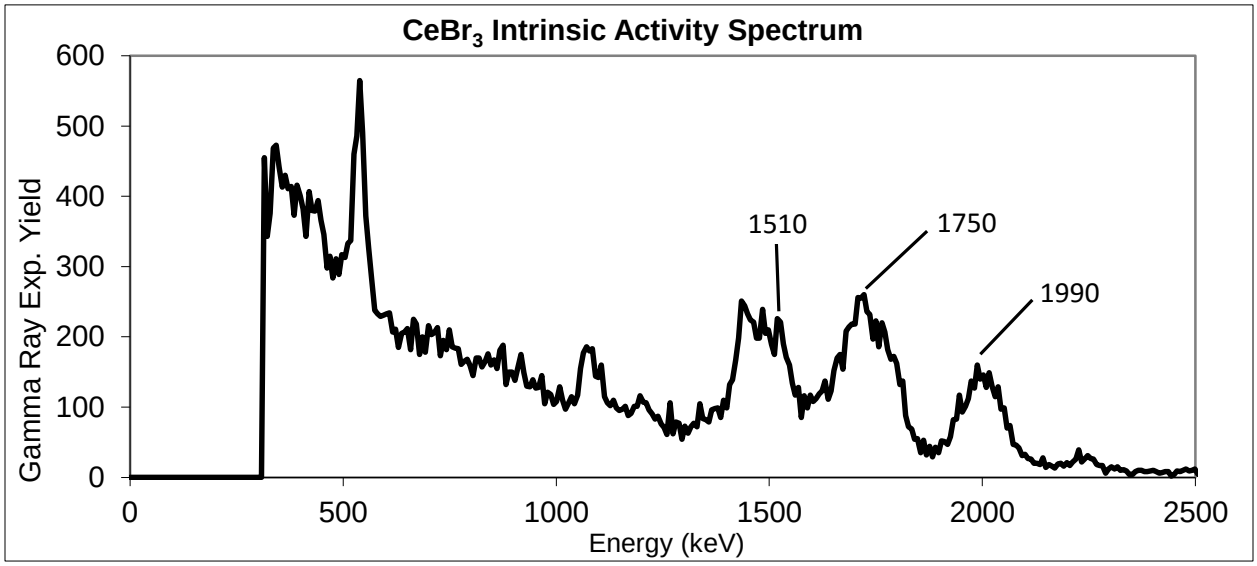

Figure 3: $CeBr_3$ Intrinsic Activity Spectrum

The intrinsic spectrum acquired in Figure 3 was originally in terms of channel number, so we have to convert this to energy by calibrating with known peaks. In Figure 4, we have displayed the full spectrum of Co-60 with its 2 characteristic peaks at 1173 and 1333 keV.

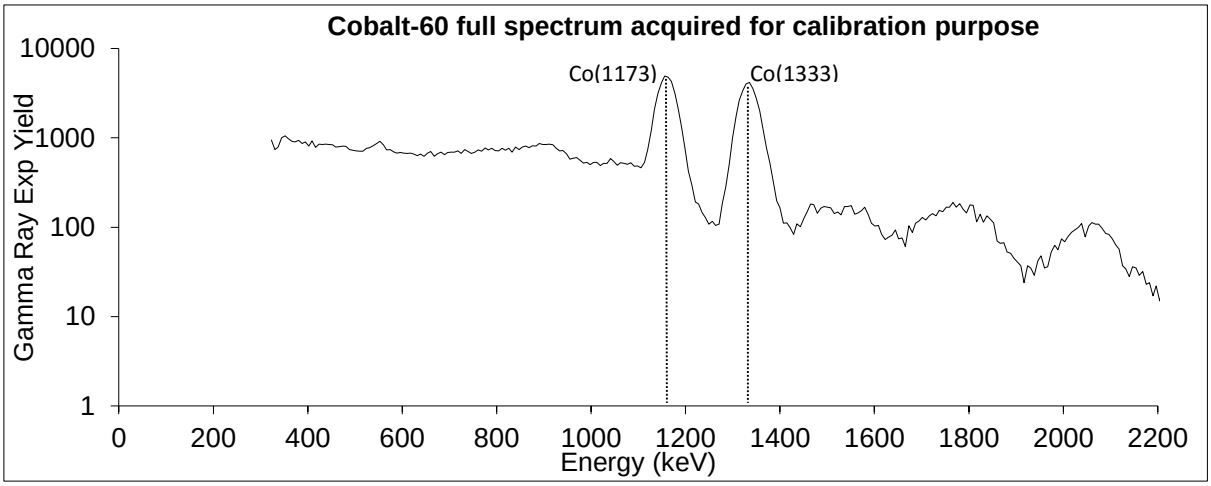

Figure 4: Full spectrum of taken with the $CeBr_3$ detector

These 2 peaks and their corresponding channel numbers are used in Figure 5 to derive the calibration ratio which is the gradient of the best-fit line and equals 6.667 keV/channel number. This number was used to convert the intrinsic spectrum in Figure 3 into an energy spectrum.

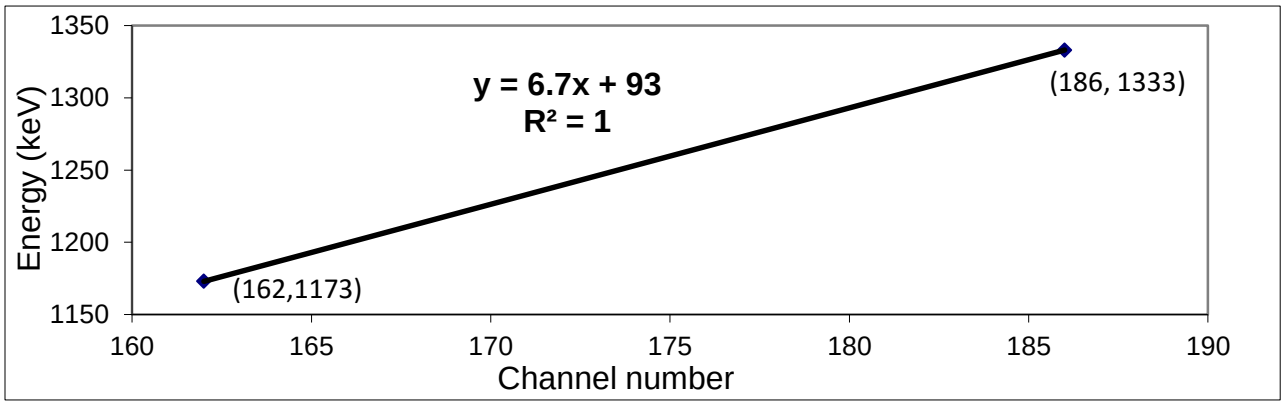

Figure 5: Calibration curve of the $CeBr_3$ detector using ^{60}Co powder

3.1.2 Activation spectrum

When the boron-contaminated water sample is exposed to the neutron beam, the detector is also exposed to the beam and emits its own prompt gamma rays due to thermal neutron capture of the detector material. The thermal gamma rays from the detector material is known as activation spectrum.

To measure the activation spectrum of the $CeBr_3$ detector, the neutron generator was operated at (70 keV, 70 μA), and no sample was placed in the cavity. Again, a run time of approximately 1500s was used. In this instance, the detector and moderator gets neutron-activated and emits prompt gamma rays which is displayed on the PC. This gives the detector activation spectrum, which includes the intrinsic spectrum and is basically the total background. The activation spectrum of our $CeBr_3$ detector is shown in Figure 6. This spectrum was taken with higher amplifier gain settings (coarse gain = 100, fine gain = 10.5) to amplify the region of 0 – 500 keV energy gamma rays. It shows capture gamma ray peaks of Br(196), Br(271), Br(367), and Br(512) from bromine and Ce(476) from cerium [8]. The emissions from activated hydrogen is in the high-energy range, hence not visible in the low-energy gamma rays we used.

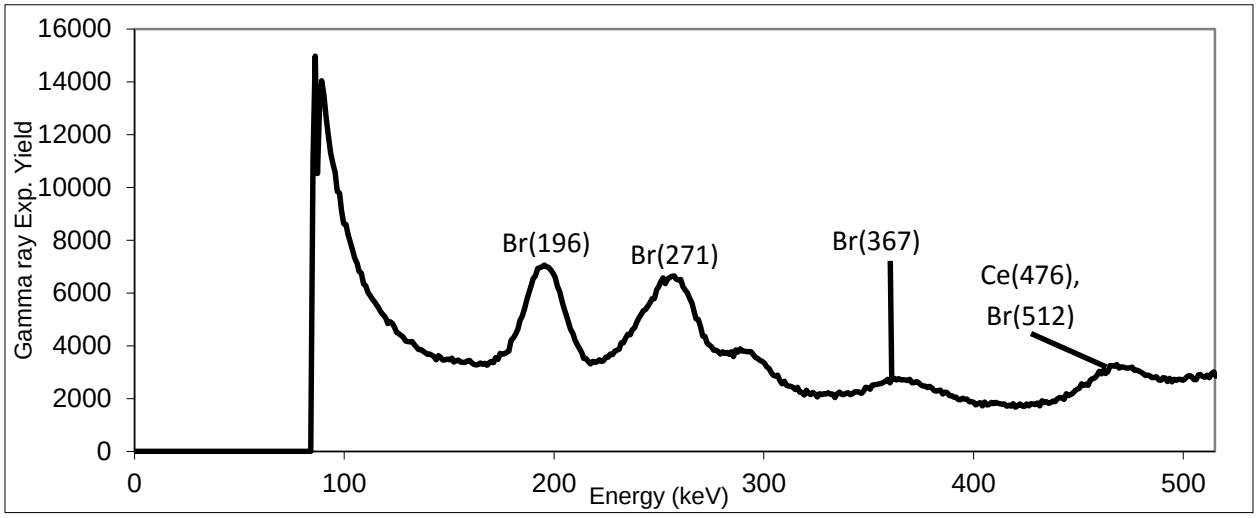

Figure 6: Thermal neutron activation spectrum of $CeBr_3$ detector

Again, the detector activation spectrum needs to be calibrated from channel number to energy units and the process is identical to the calibration for the intrinsic spectrum in Figures 3 – 5. In this case we use the Ba(356) peak located at channel 322, shown in Figure 7, together with the Br(196) peak in channel number 187 from Figure 6.

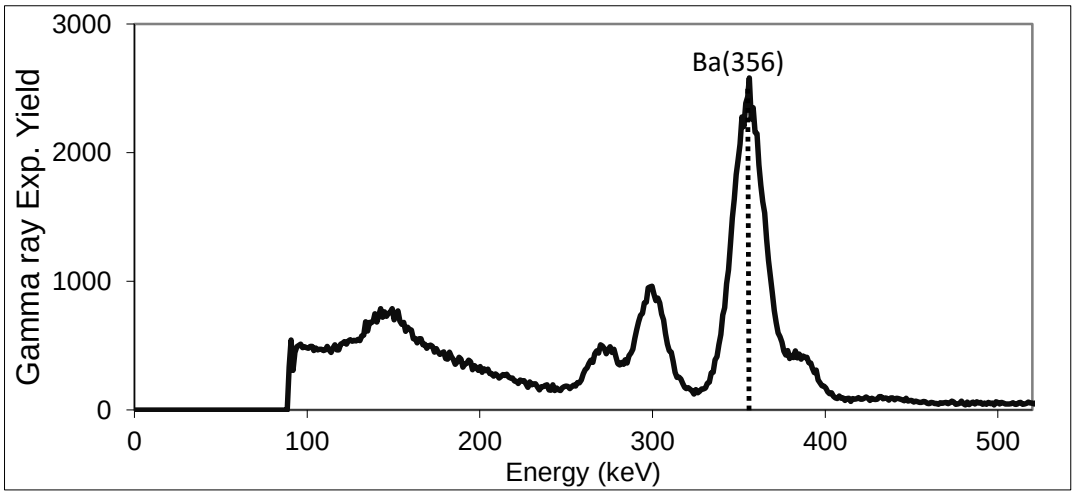

Figure 7: $CeBr_3$ detector spectrum taken with ^{133}Ba radioisotope

These 2 peaks and their corresponding channel numbers are used in Figure 8 to derive the calibration ratio which is the gradient of the best-fit line and equals 1.185 keV/channel number. This ratio was used to convert the detector activation spectrum in Figure 6 into energy spectrum.

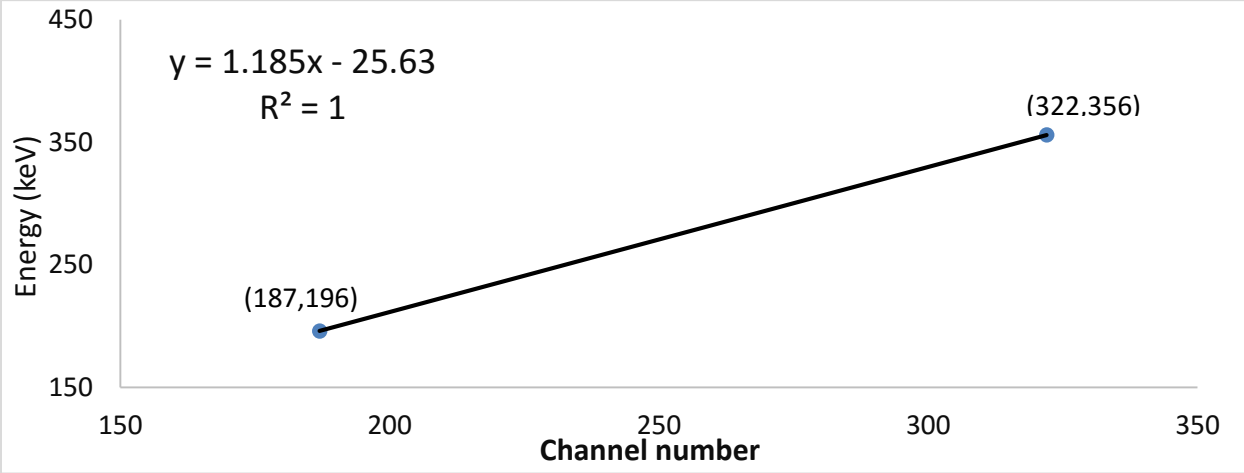

Figure 8: $CeBr_3$ detector low energy calibration curve using Br(196) and Ba(356) gamma

4. Prompt Gamma Ray Measurement from Boron-Contaminated Water Samples

To measure the sample spectrum of the boron-contaminated water samples, the bottle was inserted into the moderator cavity and the neutron beam switched on. In this case, the net boron peaks get superimposed on the detector activation spectrum to give the total sample spectrum. The difference between the detector activation spectrum and the total sample spectrum gives the net boron counts, whose area is proportional to the concentration of the boron-containing water. Performing linear regression of boron concentration against net boron counts area gives a straight line which depicts proportional relationship between the 2 variables that can be exploited for elemental composition analysis.

The experimental run time of the detector activation spectrum and total sample spectrum must correspond with each other. For instance, our former run time was 1500 s, in which case the latter must also be approximately 1500 s. Otherwise, if the background is run much longer than the sample, the background will naturally be higher than the total boron spectrum, and we will get a net depression instead of peaks! Figure 9 shows a boron spectrum superimposed upon a background spectra. This shows the effect of the boron sample whereby the B(478) peak from boron sample is superimposed upon the peaks arising from detector i.e. Ce(476) peak from cerium and Br(512) peak from bromine, both elements being present in the detector material.

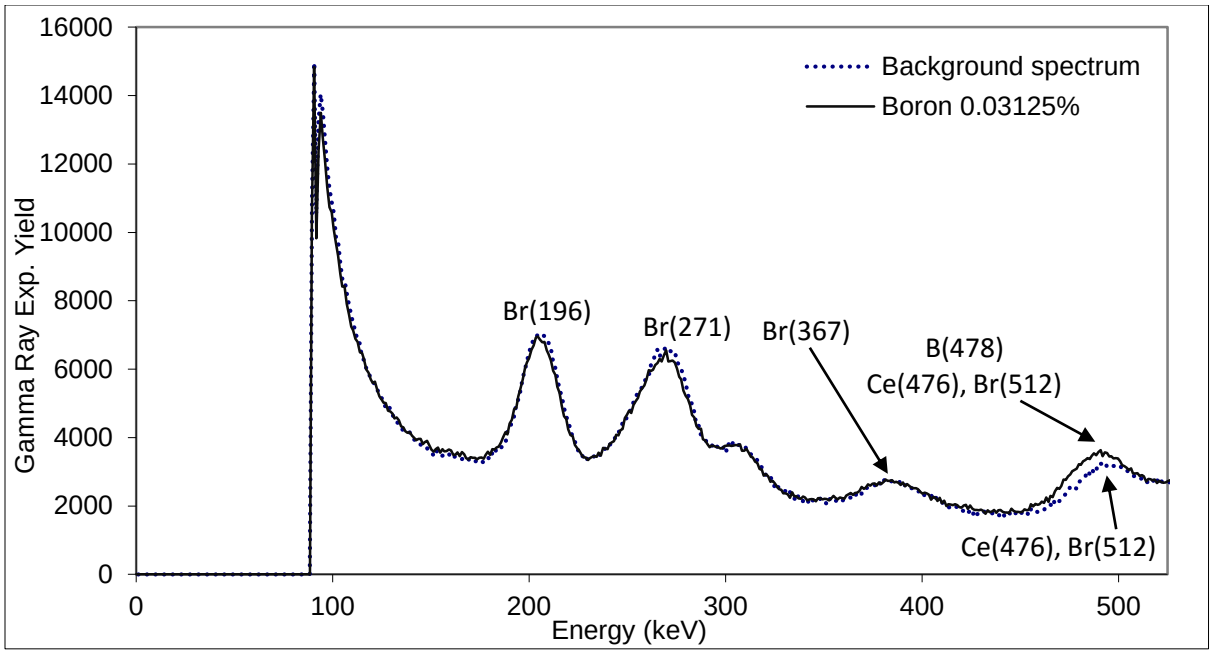

Figure 9: $CeBr_3$ detector background spectrum (dotted line) and boron spectrum (solid line)

Subsequently, prompt gamma ray spectra were recorded for five boron-contaminated water samples rated at 0.03125, 0.0833, 0.125, 0.167 and 0.25 wt% boron concentration. The spectra were recorded in PC-based data acquisition system, and plotted in Figure 10.

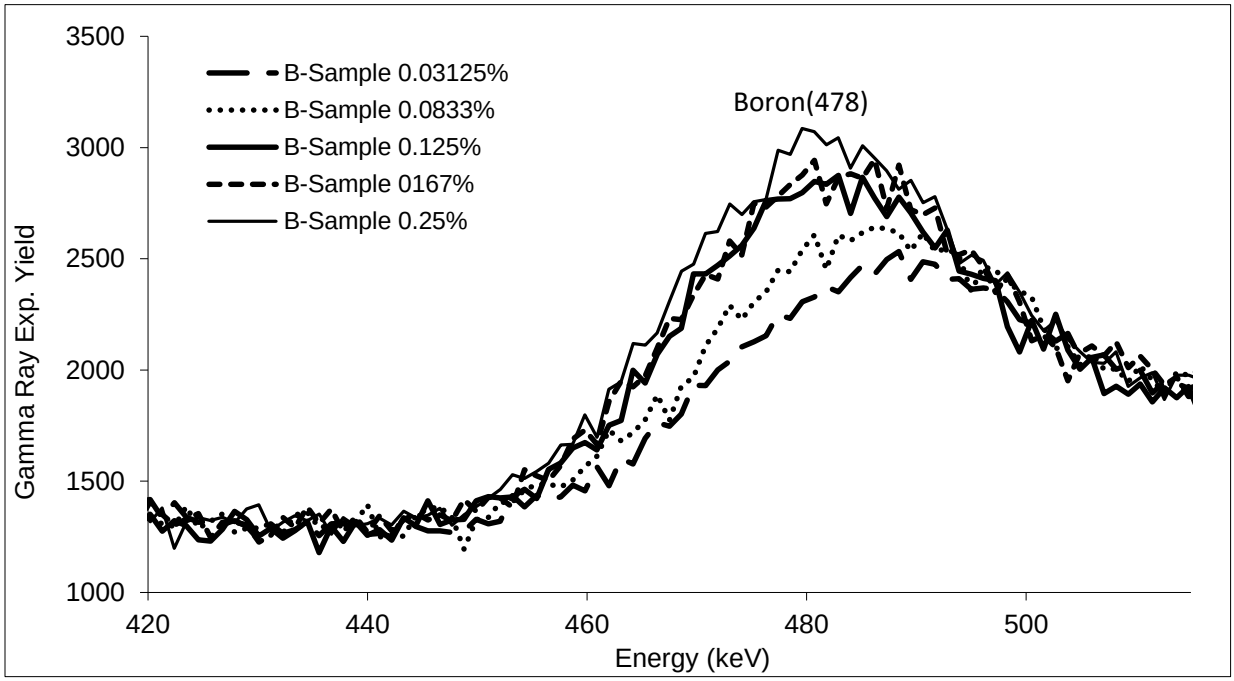

Figure 10: Sample spectra for 5 boron samples with 0.03125 – 0.25 wt% boron concentration superimposed upon each other

5. Results and Discussion

In this section, we analyse the difference spectra to determine whether the detector is performing reliably. To extract the difference spectra, the detector background spectrum is subtracted from the sample spectrum. In Figure 9, the sample spectrum is shown as a solid line and the detector background spectrum is shown as a dotted line. Figure 10 is an extension of Figure 9 showing all 5 sample spectra of 0.03125, 0.0833, 0.125, 0.167 and 0.25 wt% concentration superimposed upon each other over a gamma ray energy range of 420 – 520 keV. The spectra were recorded using a PC-based data acquisition system. From the difference between the sample spectra and the background spectrum, the difference spectra was generated as shown in Figure 11.

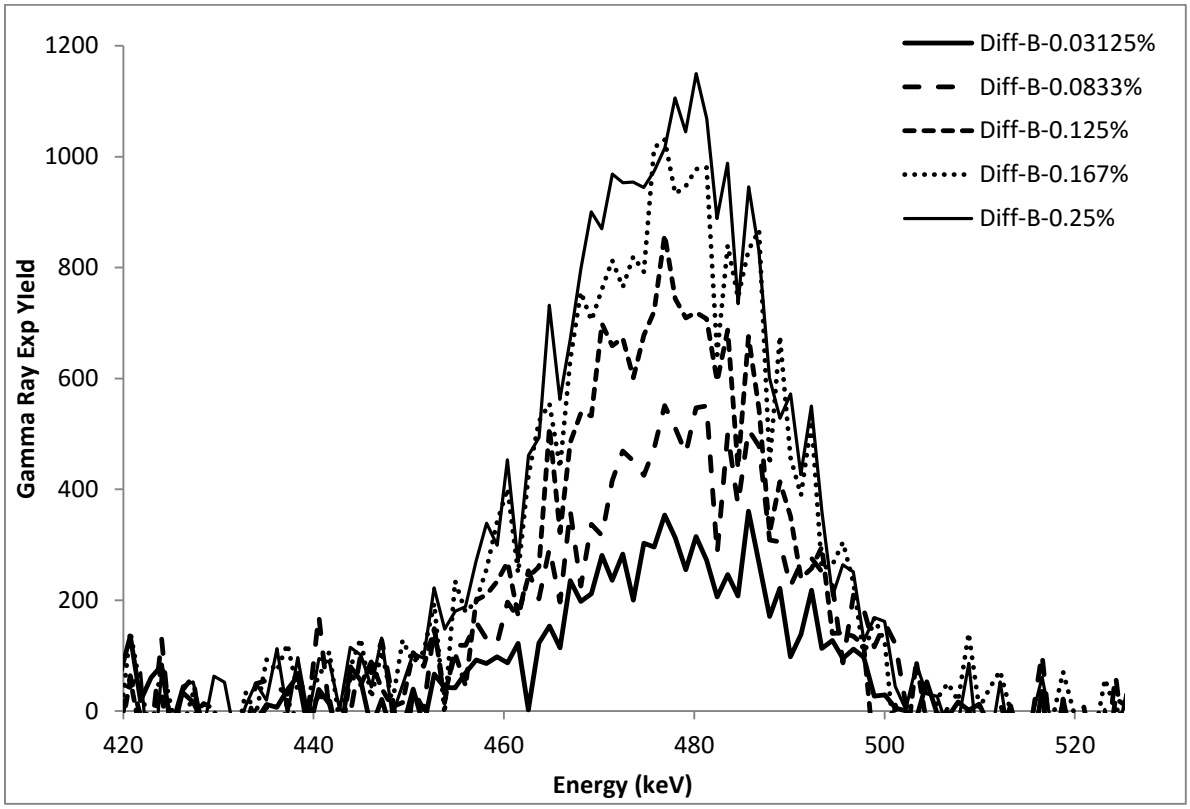

Figure 11: Difference spectra for 5 boron samples with 0.03125 – 0.25 wt% concentration boron

The area under these 5 difference spectra gives the integrated yield which is theoretically proportional to the boron concentration of the water samples. We next plot the integrated yield against boron concentration in Figure 12 to determine if our detector gives this linear relationship.

The least-squares regression line of integrated yield against boron concentration is illustrated in Figure 12 with a regression equation of y = 92570x + 0.7704 and a correlation coefficient of R = 0.98.

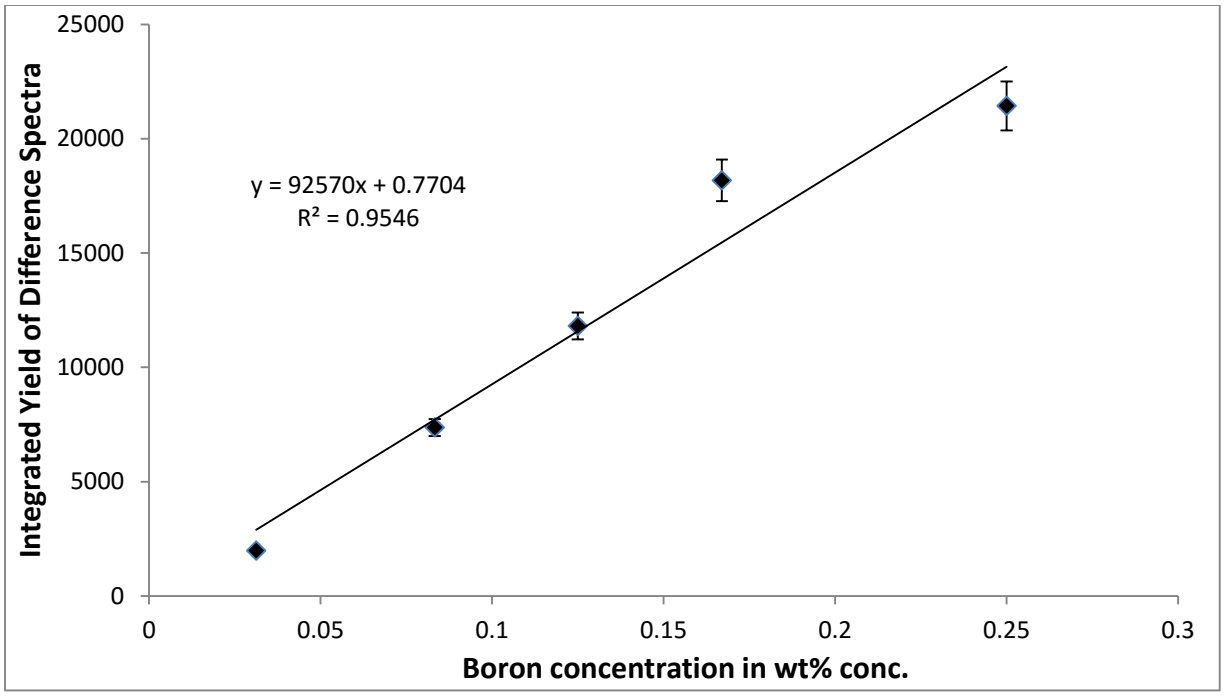

Figure 12: Plot of γ-ray intensity vs Boron wt% conc. Calibration plot

Analysing Figure 12 more closely, we notice that the 5 data points display a good scatter about the best-fit line, as evidenced by the points being close to the best fit regression line. This is an indication that only random errors (which are uncontrollable and cannot be totally eliminated) are affecting the data.

Moving on, the best-fit line generally passes through the error bars, implying the data acquired is accurate to within the limits of experimental uncertainty. It is certainly impossible to obtain data of infinite precision, so the next best alternative is to obtain data that is as accurate as possible within the limits imposed by experimental uncertainties. Having the best fit line pass close to the error bars is an indication that this has been achieved. Another indication is that the correlation coefficient of 0.98 implies very strong positive relationship between the two sets of data. Since our experimental data agrees with the theoretical proportionality relationship, we have verified that the $CeBr_3$ detector is working reliably.

Next, we discuss the practical value of the data obtained. The best-fit line is basically a calibration curve for boron. We now have a systematic procedure for testing unknown samples to determine its dissolved boron concentration. For instance, the national authorities may need polluted water to be tested for compliance to environmental legislation to ensure that its boron concentration does not exceed safety limits. We can simply test the unknown sample for its unknown Boron concentration:

$$\mathrm{B(wt\%)} = \frac{Y(478) - 0.7704}{92570}$$

where $Y(478)$ is the integrated yield of B(478) peak from Boron sample. Similar graphs and equations can be built up for other known pollutants (besides boron) and thus the techniques we have learnt in this experiment can be utilized as a strategic asset to minimize pollutant levels and optimize public health and safety.

6. Conclusion

In retrospect, this study has verified the performance of a newly-acquired $CeBr_3$ detector by comparing its performance against a theoretical principle, which states that the integrated prompt-gamma yield is proportional to the concentration of the sample tested. We chose 6 boron-containing water samples whose concentrations were in the range of 0.03125 – 0.25 wt% conc. and verified, by linear regression curve fitting, that our detector acts in compliance with the aforesaid principle, thereby proving the reliable performance of our detector. The element boron was chosen for testing due to its medical value in the boron neutron capture therapy (BNCT) treatment of certain types of cancer. Lastly, the technique used in this paper can be exploited for elemental characterization of unknown samples, which is useful in environmental pollutants and illegal materials testing, thereby demonstrating that this technique can have beneficial consequences for humanity.

7. Acknowledgements

I wish to thank Dr Akhtar Abbas Naqvi for all the assistance rendered in the completion of this experiment. In particular, mention must be made of his detailed explanations pertaining to all aspects of the experiment – both theory and experiment. I feel much enlightened on this tremendously useful technique and feel better prepared for applying this procedure in future. Shukran katseeran, duktoor!

Also, gratitude must be offered to Brother Fatai and Mr Raashid. Brother Fatai helped diligently in the technical aspects of the set-up whilst Mr Raashid – the engineer – was extremely patient in answering our repeated requests for switching the neutron gun on and off.

8. References

[1] Anderson, D. L., Belgya, T., Firestone, R. B., Kasztovsky, Z., Molnàr, G. L., Révay, Z., & Yonezawa, C. (2004). Handbook of Prompt Gamma Activation Analysis.

[2] A. M. Pollard et al. (2007). NEUTRON ACTIVATION ANALYSIS. In: Analytical Chemistry in Archaeology. pp. 123-136. [Online]. Cambridge Manuals in Archaeology. Cambridge: Cambridge University Press. Available from: Cambridge Books Online [Accessed 11 February 2016].

[3] James, W., et al. "Application of prompt gamma activation analysis and neutron activation analysis to the use of samarium as an intestinal marker."*Journal of Radioanalytical and Nuclear Chemistry* 83.2 (1984): 209-214.

[4] Knoll, Glenn F. *Radiation detection and measurement*. John Wiley & Sons, 2010.

[5] Barth, Rolf F., Albert H. Soloway, and Ralph G. Fairchild. "Boron neutron capture therapy of cancer." *Cancer Res* 50.4 (1990): 1061-1070.

[6] Quarati, F. G. A., et al. "Scintillation and detection characteristics of high-sensitivity $CeBr_3$ gamma-ray spectrometers." *Nuclear Instruments and Methods in Physics Research Section A: Accelerators, Spectrometers, Detectors and Associated Equipment* 729 (2013): 596-604.

[7] Naqvi, A. A., et al. "Pulse height tests of a large diameter fast $LaBr_3$:Ce scintillation detector." *Applied Radiation and Isotopes* 104 (2015): 224-231.

[8] Choi, H.D. et al, 2006. Database of Prompt Gamma Rays from Slow Neutron Capture for Elemental Analysis. International Atomic Energy Agency, VIENNA.